

Development of a Transferable Reactive Force Field of P/H Systems: Application to the Effect of Defects on the Mechanical Response of Black Phosphorene

Hang Xiao¹, Xiaoyang Shi¹, Feng Hao¹, Xiangbiao Liao¹, Yayun Zhang^{1,3} and Xi Chen^{1,2}

¹ *Columbia Nanomechanics Research Center, Department of Earth and Environmental Engineering, Columbia University, New York, NY 10027, USA*

² *SV Laboratory, School of Aerospace, Xi'an Jiaotong University, Xi'an 710049, China*

³ *College of Power Engineering, Chongqing University, Chongqing 400030, China*

Abstract

ReaxFF provides a method to model reactive chemical systems in large-scale molecular dynamics simulations. Here, we developed ReaxFF parameters for phosphorus and hydrogen to give a good description of the chemical and mechanical properties of pristine and defected black phosphorene. ReaxFF for P/H is transferable to a wide range of phosphorus and hydrogen containing systems including bulk black phosphorus, blue phosphorene, edge-hydrogenated phosphorene, phosphorus clusters and phosphorus hydride molecules. The potential parameters were obtained by conducting unbiased global optimization with respect to a set of reference data generated by extensive *ab initio* calculations. We extend ReaxFF by adding a 60 ° correction term which significantly improves the description of phosphorus clusters. Emphasis has been put on obtaining a good description of mechanical response of black phosphorene with different types of defects. Compared to nonreactive SW potential [1], ReaxFF for P/H systems provides a huge improvement in describing the mechanical properties the pristine and defected black phosphorene. A counterintuitive phenomenon is observed that single vacancies weaken the black phosphorene more than double vacancies with higher formation energy. Our results also show that mechanical response of black phosphorene is more sensitive to defects for the zigzag

direction than for the armchair direction. Both observations made with ReaxFF are in agreement with earlier DFT study on the defected black phosphorene under tensile strain. Since ReaxFF allows straightforward extensions to the heterogeneous systems, including oxides, nitrides, etc, ReaxFF parameters for P/H systems build a foundation for the reactive force field description of heterogeneous P systems, including P-containing 2D van der Waals heterostructures, oxides, etc.

Keywords: ReaxFF; Phosphorene; Hydrogen; 2D material; Defects; Adatoms

1. Introduction

In recent years, two-dimensional (2D) materials have attracted much interest because of their fascinating electronic, mechanical, optoelectronic, and chemical properties. Graphene [2], a single-layer of carbon atoms, has become a promising material for applications in electronics [3,4], optoelectronics [5,6] and spintronics [7]. stable and truly 2D material. The epic discovery of graphene opened up the possibility of isolating and studying the intriguing properties of a whole family of 2D materials including the 2D insulator boron nitride (BN) [8–10], 2D semiconductor molybdenum disulfide [8,11,12] and very recently, 2D phosphorus, i.e. phosphorene [13,14]. Single layer black phosphorus, i.e. phosphorene, was obtained in experiments in 2014 [14]. Because of its tunable band gap and high carrier mobility, phosphorene holds great potential in electronic and optoelectronic applications.

Over the past decade, tremendous success has been achieved in the synthesis of 2D materials. However, the cycles of synthesis, characterization and test for 2D materials are slow and costly, which inspired the development of computational tools to design new 2D materials [15–17] and to provide guidance for the fabrication of 2D devices [18–21]. Despite *ab initio* methods such as density functional theory (DFT) are able to provide accurate description of the electronic structure of 2D crystals, they are limited to small systems (several hundreds of atoms) with short time scales (picoseconds). To the contrary, molecular dynamics simulations powered by force fields are able to reach larger scale ($\gg 1000$ atoms) with longer time (beyond nanoseconds). To date, several force fields have been developed for black phosphorus.

A valence force field (VFF) for black phosphorus was first proposed in 1982 [22] and used to study the elastic properties in black phosphorus. More recently, Jiang *et al.* [1] developed a Stillinger-Weber (SW) potential for phosphorene based on the VFF model by fitting parameters were fitted to experimental phonon spectrum. For SW potential, the energy parameters are taken from the VFF model, and geometrical parameters are derived analytically from the equilibrium state of individual potential terms. While VFF model and SW potential can be used to describe phonons and elastic deformations, they are not suitable to describe states far from equilibrium

[23]. Moreover, SW potential strongly underpredicts the Young's modulus of black phosphorene in the zigzag direction [24]. Due to its nonreactive nature, SW potential has difficulty describing phosphorene with defects. In 2001, van Duin *et al.* developed a reactive force field (ReaxFF) for hydrocarbons [25]. ReaxFF is a bond order interaction model, capable of handling bond breaking and forming with associated changes in atomic hybridization. Since its development, ReaxFF model has been applied to a wide range of systems [26–32].

Here we develop a ReaxFF parameter set for P and H to describe chemical and mechanical properties of pristine and defected black phosphorene. ReaxFF for P/H is transferable to a wide range of phosphorus and hydrogen containing systems including bulk black phosphorus, blue phosphorene, hydrogenated phosphorene, phosphorus clusters and phosphorus hydride molecules. The ReaxFF parameters for P/H were fitted to a set of reference data generated by extensive ab initio calculations. ReaxFF was extended by a 60 °correction term which significantly improves the description of phosphorus clusters. ReaxFF for P/H provides a huge improvement in describing the mechanical properties the pristine and defected black phosphorene over the SW potential. The ReaxFF parameters for P/H presented here provide a first step in the development of a reactive force field description for heterogeneous P systems.

2. Methodology

2.1 DFT Calculations

The fitting data used for P/H systems was obtained from DFT calculations performed with the Cambridge series of total-energy package (CASTEP) [33,34]. For these calculations, ultrasoft pseudopotentials were used to describe the core electrons and the electron exchange-correlation effects was described by the Perdew–Burke–Ernzerhof (PBE) [35] generalized gradient approximation. In this work, the empirical dispersion correction schemes proposed by Grimme (D2) [36] was used in combination with PBE functional. In computing the energies of phosphorus clusters, phosphorus hydride molecules and phosphorene with defects and adatoms, spin polarization was used to account for the energy contributions from magnetization. Periodic

boundary conditions were used for all the calculations, with monolayer structures represented by a periodic array of slabs separated by a 15 Å thick vacuum region. A large 5×7 supercell of black phosphorene is adopted to study the effect of defects and adatoms. A plane wave cutoff of 520 eV was used to determine the self-consistent charge density. For condensed phases, Brillouin zone integrations were performed with Monkhorst-Pack [37] mesh with 0.02 Å^{-1} k -point spacing. For cluster calculations, a cubic supercell of 20 Å (to ensure the interactions between clusters in adjacent cells is negligible) was used with the clusters or molecules placed at the center of the cell with Brillouin zone sampled at the Γ point. All geometries have been optimized by CASTEP using the conjugate gradient method (CG) with convergence tolerances of a total energy within $5.0 \times 10^{-6} \text{ eV atom}^{-1}$, maximum Hellmann–Feynman force within 0.01 eV Å^{-1} , maximum ionic displacement within $5.0 \times 10^{-5} \text{ Å}$, and maximum stress within 0.01 GPa. For black phosphorene, the stress-strain response in the armchair and zigzag directions were calculated using the method described in the references [38,39] with CASTEP. The CASTEP calculations show good agreement with previous theoretical values for a variety of phosphorene properties: lattice constants [14], Young’s modulus in the armchair and zigzag directions [40], formation energies of defects [41] and adatoms [42]. And the calculated lattice constants of bulk black phosphorus agree well with experimental values [43].

2.2 ReaxFF

The ReaxFF model [25–27] is a bond-order interaction model. For ReaxFF, the interatomic potential describes chemical reactions through a bond-order framework, in which bond order is directly calculated from interatomic distances. Within the bond order framework, electronic interactions, the driving force of the chemical bonding, are treated implicitly, allowing the method to simulate chemical reactions without expensive quantum chemical calculations. Typical empirical force field (EFF) potentials adopt empirical equations to describe bond stretching, bond bending, and bond torsion events, with additional expressions to handle van der Waals (vdW) and Coulomb interactions. EFF potentials require a user-specified connectivity table, while ReaxFF is able to calculate the atom connectivity on the fly, which separates

ReaxFF from EFF potentials in that the breaking and forming of bonds can be captured during MD simulations.

For a ReaxFF description of P/H systems, the bond energies (E_{bond}) are corrected with over-coordination penalty energies (E_{over}). Energy contributions from valence angle (E_{val}) and torsion angle (E_{tor}) are included. Dispersion interactions are described by the combination of the original van der Waals term (E_{vdw}) and low-gradient vdW correction term (E_{lgvdw}) [30]. Energy contribution from Coulomb interactions ($E_{Coulomb}$) are taken into account between all atom pairs, where the atomic charges are calculated based on connectivity and geometry using the Electron Equilibration Method (EEM) [44]. All energy terms except the last three are bond-order dependent and a detailed description of them (except E_{60cor}) can be found in Refs. [25,26,30]. The total energy is the summation of these energy pieces, shown by

$$E_{system} = E_{bond} + E_{over} + E_{val} + E_{60cor} + E_{tors} + E_{vdw} + E_{lgvdw} + E_{Coulomb} \quad (1)$$

The stability of P₄ cluster and the instability of larger phosphorus clusters was a continuing puzzle for several decades [45]. The phosphorus is often expected to favor valence angles near 101 ° [46]. If this is true, the strain energy of bonds in P₄ cluster (with 60 ° valence angles) should make it unstable. This problem has been addressed by including the effect of d-orbitals in QM calculations [47]. It is thus impossible for ReaxFF to describe the stability of the P₄ cluster (and other phosphorus clusters with valence angles near 60 °) while providing a good description of condensed phases of phosphorus at the same time. To address this problem, we added a 60 ° angle correction term to the Eq. 1.

$$E_{60cor} = -p_{cor1} \cdot f_1(BO_{ij}) \cdot f_2(BO_{jk}) \cdot \exp \left[-p_{cor2} * (\theta_{60} - \theta_{ijk})^2 \right] \quad (2a)$$

$$f_1(BO_{ij}) = 1 - \exp(-p_{val3} \cdot BO_{ij}^{p_{cor3}}) \quad (2b)$$

$$f_2(BO_{jk}) = 1 - \exp(-p_{val3} \cdot BO_{jk}^{p_{cor3}}) \quad (2c)$$

In section 3.2.2, we will see that the accuracy of cluster formation energies is significantly improved by adding 60 ° angle correction term to the total energy function.

LAMMPS code [48] was used to perform MD calculations for the tensile behavior for the black phosphorene of dimension $27.5 \times 25.8 \text{ \AA}$ at 1.0 K and 300.0 K. Periodic boundary conditions were employed in both the zigzag and armchair directions. The equation of motion was solved with a velocity Verlet algorithm, using a time step of 1.0 fs, which led to stable dynamics trajectories. The system was thermalized to steady state with the NPT (constant number of particles, constant pressure, and constant temperature) ensemble for 50 ps by the Nosé-Hoover [49,50] thermostat. Subsequently, the black phosphorene was stretched in zigzag or armchair direction at a strain rate of 10^9 s^{-1} , and the stress in the lateral direction was fully relaxed. In computing the stress, inter-layer space of 5.24 \AA was used as the thickness of the black phosphorene. The Young's modulus was calculated from the stress-strain curve in the strain range $[0, 0.01]$. Following the same procedure of calculating the stress-strain curve for the defect-free black phosphorene, the MD calculations for defected phosphorene under tensile strain were conducted for the black phosphorene of dimension $27.5 \times 25.8 \text{ \AA}$ at 1.0 K with one defect (single vacancy, double vacancy or Stone-Wales defect).

An important technical note: for the simulation of P/H systems with the 60° angle correction, one needs to recompile the LAMMPS package with our modified source file, *reaxc_valence_angles.cpp*. Note that we have tested that 60° angle correction will only affect the properties of P/H systems with valence angles near 60° . Thus for the simulation of condensed phases (either pristine or defected) and phosphorus hydride molecules, one can simply use the original version of LAMMPS package.

3. Results and Discussions

3.1 DFT Training of Force Field

The ReaxFF parameters for P/H systems were optimized using a modified version of the evolutionary algorithms (EA) software suite OGOLEM [51,52], which is able to globally optimize ReaxFF parameter sets with high parallel efficiency. Based on DFT calculations for

bulk black phosphorus, pristine and defected black phosphorene, blue phosphorene, phosphorus hydride molecules and phosphorus clusters, ReaxFF parameters were generated for P-P and P-H bond energies, P-P-P, H-P-P and H-P-H valence angle energies and for H-P-P-P and H-P-P-H torsion energies.

The parametrization of ReaxFF for P/H systems consisted of following steps, briefly mentioned in the introduction.

- (i) Training set of DFT data points was built for crystals, clusters and phosphorus hydride molecules. For the crystal phases, data of the energy dependence on volume of the black phosphorus crystal and on in-plane area of both black and blue phosphorene. Bond dissociation profiles of P-P bonds in the P_2H_4 and P_2H_2 molecules (Fig. 4(c)), and of P-H bonds in the PH_3 molecules (Fig. 4(a)) were included. Energy profiles for angle distortion of P-P-P in the P_3H_5 molecule (Fig. 4(e)), of H-P-P in the P_2H_4 molecule (Fig. 4(b)), and of H-P-H in the PH_3 molecule (Fig. 4(a)) were added. In these energy profiles, only the lowest-energy states (singlet, triplet or quintet depending on geometry) were included. Mulliken charges for the phosphorus hydride molecules were added to the training set. A minimum number of terms in Eq. 1 were selected (starting with E_{bond} , E_{over} , E_{val} , E_{vdw} , $E_{Coulomb}$). The parameters were fitted to the training set using OGOELM [51,52].
- (ii) The torsion angle term (E_{tor}), low gradient correction term (E_{lgvdw}) and 60 ° angle correction term (E_{60cor}) were added to the total energy function to obtain a refined fit to the training set. Energy profiles for torsion distortion of H-P-P-H in the P_2H_4 molecule and of H-P-P-P in the P_4H_2 molecule were included. Energies and geometries of phosphorene with different types of defects were added to the training set.
- (iii) The global optimized parameters were validated by the comparison of properties calculated by ReaxFF to experimental and DFT data.

3.2 Parameterization and Validation of ReaxFF

Our final fitted ReaxFF for P/H systems is given in Tables 1-7. The potential form was given in Eq. 1 (a detailed description of all terms can be found in Refs. [25,26,30]). Unless otherwise stated, all ReaxFF results in the following discussion refer to our global optimized ReaxFF parameter set.

3.2.1 Relative stabilities for bulk black phosphorus, black and blue phosphorene

For ReaxFF to accurately describe phosphorus in the condensed phase, descriptions for different crystalline phases should be included in the DFT training set. Relative stabilities of the black phosphorus crystal as a function of unit cell volumes and relative stabilities of the both black and blue phosphorene as a function of unit cell in-plane areas were calculated for use in the training set for the ReaxFF parameterization.

ReaxFF model gives a good description of lattice parameters of all three crystal phases (see Table 8) and a good description of the crystal structures of these crystal phases (see Fig. 1). DFT results and ReaxFF results of cohesive energies are compared to SW results and experimental data in Table 9. The equilibrium cohesive energy of bulk phosphorus used in the fitting procedure was taken as the experimental data [53] of -3.26 eV rather than the value computed from DFT of -3.43 eV. ReaxFF predicts a black phosphorus cohesive energy of -2.91 eV. The cohesive energy of black phosphorene calculated by ReaxFF is -2.84 eV, which slightly underestimates the DFT result of -3.35 eV. Still, ReaxFF provides a much better prediction of cohesive energy of phosphorene than SW potential, which yields a cohesive energy of -0.54 eV. ReaxFF are able to correctly reproduce the relative order of stability of three crystal phases (shown in Table 9). In Fig. 2(a) and Fig. 2(b), we see that ReaxFF correctly describes the relative stabilities of bulk black phosphorus for a broad range of cell volume and black phosphorene for a broad range of cell area. In the training set, not all the data can be fitted equally well. For blue phosphorene (Fig. 2(c)), ReaxFF slightly overestimates the in-plane area of the unit cell, leading

to a small offset of the energy profile of the relative stability. Our focus in this paper is on the properties of black phosphorene, so the lack of agreement for blue phosphorene is not critical.

3.2.2 Relative stabilities of phosphorus clusters

For ReaxFF to provide accurate description of phosphorus in clusters, the geometries and formation energies of P clusters of sizes 4,5,6 and 8 atoms are included in the training set. The formation energies per atom of clusters, E_{cf} , defined by

$$E_{cf} = E_c/n - E_{cohesive}(\text{bulk}) \quad (3)$$

Where E_c is the energy of the relaxed phosphorus cluster with n atoms, $E_{cohesive}(\text{bulk})$ is the cohesive energy of the bulk black phosphorus. As can be seen from Fig. 3 ReaxFF is able to provide a very good description of the geometries of P clusters. Table 10 shows that the cluster formation energies per atom calculated by ReaxFF with 60 ° correction agree well with the DFT results. It is intriguing that a simple 60 ° angle correction term is able to provide such a huge improvement in terms of cluster formation energies.

3.2.3 Potential energy curves for phosphorus hydride molecules

Data for selected phosphorus hydride molecules was also included in the training set to train the P-H interactions and to enhance the transferability of the ReaxFF for P/H systems. To include DFT data for P-H, P-H bonds, dissociation profiles were determined from DFT calculations for phosphine, P_2H_2 and P_2H_4 molecules. The bond dissociation profiles were generated from the equilibrium geometries of these molecules by changing the bond length from the equilibrium value while allowing other structural parameters to relax, which are shown in Fig. 4 (a-c). Only the lowest-energy states (singlet, triplet or quintet depending on geometry) were included in bond dissociation profiles. The DFT and ReaxFF curves are shown in Fig. 4 (a-c).

To include DFT data for P-P-P, H-P-P and H-P-H valence angles, P_3H_5 , P_2H_2 and phosphine molecules were used, respectively. Following the same procedure of constructing the bond dissociation profiles, P_3H_5 , P_2H_2 and phosphine molecules were geometry optimized to create reference states. Afterwards the valence angles were modified while other structural parameters were optimized. The resulting angle distortion curves are shown in Fig. 5(d-f).

Energy profiles for torsion distortion of H-P-P-H in the P_2H_4 molecule and of H-P-P-P in the P_4H_2 molecule were also included in the training set. The torsion distortion curves were generated from the equilibrium geometries of these molecules by changing the relevant torsion angle from the equilibrium value while allowing other structural parameters to relax, which are shown in Fig. 4 (g-h).

In Fig. 4 (a, d, f, g, h), it is visible that the interactions between phosphorus and hydrogen atoms in phosphorus hydride molecules are well reproduced with ReaxFF. For the interactions between phosphorus atoms in phosphorus hydride molecules (see Fig. 4 (b, c, e)), agreement between the ReaxFF and DFT results are not perfect, due to crystal phases of phosphorus were in general prioritized over the phosphorus hydride molecules. The depth of the ReaxFF potential well in Fig. 4(b) is shallow, in order to balance the errors in cohesive energy for bulk black phosphorus (cf. Table 9) and the ultimate strength of black phosphorene in zigzag direction (cf. Fig. 7).

3.2.4 Defect formation energies for black phosphorene

Properties and applications of 2D materials are strongly affected by defects [54], which are generally induced by irradiations of ion or electron [55]. Defect engineering has emerged as an important approach to modulate the properties of 2D materials. Thus the accurate description of behavior of different types of defects in phosphorene is critical for ReaxFF of P/H systems. The structures and formation energies of single vacancy (SV), double vacancy (DV) and Stone-Wales (SW) defects are included in the training set. The defect formation energy, E_{df} , defined by

$$E_{df} = E_d - E_{cohesive}(\text{black}) \cdot n \quad (4)$$

Where E_d is the energy of the defected phosphorene (geometry optimized) with n phosphorus atoms, $E_{cohesive}(\text{black})$ is the energy per atom of the black phosphorene. Fig. 5 shows that ReaxFF performs very well at predicting defects geometries of all three types as compared with DFT calculations. And SW potential fails in predicting the structure of all three type of defects. In Table 11, it can be seen that ReaxFF provides a good description of the defect formation

energy of single vacancy in phosphorene and the relative stability between single vacancy and double vacancy. The formation energies of double vacancy and Stone-Wales defect are overestimated by roughly 30% by ReaxFF. For SW potential, the formation energies of single and double vacancy are seriously underestimated (see Table 11) and the Stone-Wales defect is unstable (see Fig. 5), leading to an erroneous 0 eV formation energy. Compared to SW potential, ReaxFF provides a huge improvement in describing different types of defects in phosphorene.

3.2.5 Transferability test: adatom binding energies for black phosphorene

Due to its 2D nature, black phosphorene nanosheet always has larger surface area to volume ratio than that of the bulk black phosphorus, leading to a high chemical activity to foreign atoms. Thus the accurate description of surface adatoms in phosphorene is important for ReaxFF. Structures and formation energies of phosphorus and hydrogen adatoms for black phosphorene were withheld from the training set, to serve as validation data. Fig. 6 shows that ReaxFF agrees very well with DFT calculations at predicting adsorption structures of P and H adatoms. In Table 11, it can be seen that ReaxFF provides a very good description of the binding energy of H adatom and slightly underestimates the binding energy of P adatom. Overall, ReaxFF is able to give a good description of P and H adatoms on black phosphorene. Since structures and formation energies of P and H adatoms for black phosphorene are not included in the training set, these results indicate the transferability of the ReaxFF for P/H systems.

3.3 Mechanical Property Predictions of Black Phosphorene from ReaxFF

In Table 13, Young's modulus of black phosphorene in armchair and zigzag directions calculated by ReaxFF and SW potential are compared to DFT results. ReaxFF performs fairly well in reproducing the Young's modulus of black phosphorene in both directions, while SW potential underestimates the Young's modulus of black phosphorene in both directions. Fig. 7 shows the stress-strain curves of black phosphorene in zigzag and armchair directions calculated with DFT, ReaxFF and SW potential. For zigzag direction, ReaxFF is able to capture the modulus change as the strain increases, providing a reasonable agreement in ultimate strength

and failure strain. SW potential severely underestimates the ultimate strength and failure strain in the zigzag direction. For armchair direction, ReaxFF overpredicts the failure strain while SW potential underpredicts it. The ultimate strength of black phosphorene in the armchair direction is slightly overestimated by ReaxFF, while it is severely underestimated by SW potential. ReaxFF yields smaller failure strain at 300 K than 1.0 K for both the zigzag and armchair directions (see Fig. 8). Generally, ReaxFF gives a better representation of mechanical response of pristine black phosphorene compared to SW potential.

3.4 Effect of Defects on the Mechanical Response of Black

Phosphorene

Stress-strain curves of defected black phosphorene in the zigzag and armchair directions calculated with ReaxFF at 0 K are shown in Fig. 9 and Fig. 10, respectively. For armchair direction, black phosphorene with single vacancies shows a larger reduction in the failure strain than black phosphorene with double vacancies (keeping defect density the same), even though double vacancy has higher formation energy than single vacancy. The reduction in the failure strain induced by Stone-Wales defect is in between that of single and double vacancy. Only minor reduction in Young's modulus in the armchair direction is induced by all three types of defects.

For zigzag direction, all three types of defects reduce the failure by more or less 50%. It can be seen that defects lead to larger reduction of Young's modulus in the armchair direction, compared to the zigzag direction scenarios. Thus, the mechanical response of black phosphorene is more sensitive to defects for the zigzag direction than for the armchair direction.

Hao *et al.* [56] conducted first-principles study of the effect of single and double vacancies on the mechanical response of black phosphorene. Intriguingly, the effect of single and double vacancies on the mechanical response of black phosphorene in both armchair and zigzag directions predicted by ReaxFF agrees fairly well with DFT results [56]. This clearly shows that ReaxFF for P/H systems provides a robust tool to study the effect of defects on the mechanical response of black phosphorene on a much larger space and time scale compared to DFT.

4. Concluding Remarks

The present work presents a reactive force field (ReaxFF) for phosphorus and hydrogen developed to give an accurate description of the chemical and mechanical properties of pristine and defected black phosphorene. ReaxFF for P/H is transferable to a wide range of P/H systems including bulk black phosphorus, blue phosphorene, phosphorus clusters and phosphorus hydride molecules. We extend ReaxFF by adding a 60° correction term which significantly improves the description of phosphorus clusters. Emphasis has been put on obtaining a good description of mechanical response of black phosphorene with different types of defects. Compared to SW potential, ReaxFF for P/H systems provides a huge improvement in describing the cohesive energy, mechanical response and different types of defects of black phosphorene. We observe a counterintuitive phenomenon that single vacancies weaken the black phosphorene more than relatively more unstable double vacancies. It is shown that mechanical response of black phosphorene is more sensitive to defects for the zigzag direction than for the armchair direction. Both observations made with ReaxFF are in agreement with earlier first-principle study on the defected black phosphorene under tensile strain. Straightforward extensions to the heterogeneous systems, including oxides, nitrides, etc, enable the ReaxFF parameters for P/H systems to build a solid foundation for the simulation of a wide range of P-containing materials.

Acknowledgments

The study is supported by the National Natural Science Foundation of China (11172231), DARPA (W91CRB-11-C-0112), and AFOSR (FA9550-12-1-0159).

References

- [1] Jiang J-W 2015 Parametrization of Stillinger–Weber potential based on valence force field model: application to single-layer MoS₂ and black phosphorus *Nanotechnology* **26** 315706

- [2] Novoselov K S, Geim A K, Morozov S V, Jiang D, Katsnelson M I, Grigorieva I V, Dubonos S V and Firsov A A 2005 Two-dimensional gas of massless Dirac fermions in graphene *Nature* **438** 197–200
- [3] Geim A K and Novoselov K S 2007 The rise of graphene *Nat. Mater.* **6** 183–191
- [4] De Heer W A, Berger C, Wu X, First P N, Conrad E H, Li X, Li T, Sprinkle M, Hass J, Sadowski M L and others 2007 Epitaxial graphene *Solid State Commun.* **143** 92–100
- [5] Bonaccorso F, Sun Z, Hasan T and Ferrari A 2010 Graphene photonics and optoelectronics *Nat. Photonics* **4** 611–622
- [6] Bao Q and Loh K P 2012 Graphene photonics, plasmonics, and broadband optoelectronic devices *ACS Nano* **6** 3677–3694
- [7] Rao C N R, Sood A K, Subrahmanyam K S and Govindaraj A 2009 Graphene: The New Two-Dimensional Nanomaterial *Angew. Chem. Int. Ed.* **48** 7752–77
- [8] Novoselov K S, Jiang D, Schedin F, Booth T J, Khotkevich V V, Morozov S V and Geim A K 2005 Two-dimensional atomic crystals *Proc. Natl. Acad. Sci. U. S. A.* **102** 10451–3
- [9] Pacil éD, Meyer J C, Girit Ç Ö and Zettl A 2008 The two-dimensional phase of boron nitride: Few-atomic-layer sheets and suspended membranes *Appl. Phys. Lett.* **92** 133107
- [10] Topsakal M, Aktürk E and Ciraci S 2009 First-principles study of two- and one-dimensional honeycomb structures of boron nitride *Phys. Rev. B* **79** 115442
- [11] Mak K F, Lee C, Hone J, Shan J and Heinz T F 2010 Atomically Thin MoS_2 : A New Direct-Gap Semiconductor *Phys. Rev. Lett.* **105** 136805
- [12] Radisavljevic B, Radenovic A, Brivio J, Giacometti V and Kis A 2011 Single-layer MoS_2 transistors *Nat. Nanotechnol.* **6** 147–50
- [13] Li L, Yu Y, Ye G J, Ge Q, Ou X, Wu H, Feng D, Chen X H and Zhang Y 2014 Black phosphorus field-effect transistors *Nat. Nanotechnol.* **9** 372–7
- [14] Liu H, Neal A T, Zhu Z, Luo Z, Xu X, Tománek D and Ye P D 2014 Phosphorene: An Unexplored 2D Semiconductor with a High Hole Mobility *ACS Nano* **8** 4033–41
- [15] Glass C W, Oganov A R and Hansen N 2006 USPEX—evolutionary crystal structure prediction *Comput. Phys. Commun.* **175** 713–720
- [16] Lyakhov A O, Oganov A R, Stokes H T and Zhu Q 2013 New developments in evolutionary structure prediction algorithm USPEX *Comput. Phys. Commun.* **184** 1172–82

- [17] Wang Y, Lv J, Zhu L and Ma Y 2012 CALYPSO: A method for crystal structure prediction *Comput. Phys. Commun.* **183** 2063–70
- [18] Kumar H, Er D, Dong L, Li J and Shenoy V B 2015 Elastic Deformations in 2D van der Waals Heterostructures and their Impact on Optoelectronic Properties: Predictions from a Multiscale Computational Approach *Sci. Rep.* **5** 10872
- [19] Kumar H, Dong L and Shenoy V B 2016 Limits of Coherency and Strain Transfer in Flexible 2D van der Waals Heterostructures: Formation of Strain Solitons and Interlayer Debonding *Sci. Rep.* **5**
- [20] Khorshidi A and Peterson A A 2016 Amp: A modular approach to machine learning in atomistic simulations *Comput. Phys. Commun.* **207** 310–24
- [21] Midtvedt D, Lewenkopf C H and Croy A 2017 Multi-scale approach for strain-engineering of phosphorene *ArXiv170106395 Cond-Mat*
- [22] Kaneta C, Katayama-Yoshida H and Morita A 1982 Lattice dynamics of black phosphorus *Solid State Commun.* **44** 613–617
- [23] Jiang J-W, Park H S and Rabczuk T 2013 Molecular dynamics simulations of single-layer molybdenum disulphide (MoS₂): Stillinger-Weber parametrization, mechanical properties, and thermal conductivity *J. Appl. Phys.* **114** 064307
- [24] Midtvedt D and Croy A 2016 Comment on “Parametrization of Stillinger–Weber potential based on a valence force field model: application to single-layer MoS₂ and black phosphorus” *Nanotechnology* **27** 238001
- [25] van Duin A C T, Dasgupta S, Lorant F and Goddard W A 2001 ReaxFF: A Reactive Force Field for Hydrocarbons *J. Phys. Chem. A* **105** 9396–409
- [26] van Duin A C T, Strachan A, Stewman S, Zhang Q, Xu X and Goddard W A 2003 ReaxFFSiO Reactive Force Field for Silicon and Silicon Oxide Systems *J. Phys. Chem. A* **107** 3803–11
- [27] Zhang Q, Çağın T, van Duin A, Goddard W A, Qi Y and Hector L G 2004 Adhesion and nonwetting-wetting transition in the $\text{Al}/\text{Al}_2\text{O}_3$ interface *Phys. Rev. B* **69** 045423
- [28] Ojwang’ J G O, Santen R van, Kramer G J, Duin A C T van and Iii W A G 2008 Predictions of melting, crystallization, and local atomic arrangements of aluminum clusters using a reactive force field *J. Chem. Phys.* **129** 244506

- [29] LaBrosse M R, Johnson J K and van Duin A C T 2010 Development of a Transferable Reactive Force Field for Cobalt *J. Phys. Chem. A* **114** 5855–61
- [30] Liu L, Liu Y, Zybin S V, Sun H and Goddard W A 2011 ReaxFF-*lg*: Correction of the ReaxFF Reactive Force Field for London Dispersion, with Applications to the Equations of State for Energetic Materials *J. Phys. Chem. A* **115** 11016–22
- [31] Singh S K, Srinivasan S G, Neek-Amal M, Costamagna S, van Duin A C T and Peeters F M 2013 Thermal properties of fluorinated graphene *Phys. Rev. B* **87** 104114
- [32] Mortazavi B, Ostadhossein A, Rabczuk T and van Duin A C T 2016 Mechanical response of all-MoS₂ single-layer heterostructures: a ReaxFF investigation *Phys Chem Chem Phys* **18** 23695–701
- [33] Segall M D, Lindan P J D, Probert M J, Pickard C J, Hasnip P J, Clark S J and Payne M C 2002 First-principles simulation: ideas, illustrations and the CASTEP code *J. Phys. Condens. Matter* **14** 2717
- [34] Payne M C, Teter M P, Allan D C, Arias T A and Joannopoulos J D 1992 Iterative minimization techniques for *ab initio* total-energy calculations: molecular dynamics and conjugate gradients *Rev. Mod. Phys.* **64** 1045–97
- [35] Perdew J P, Burke K and Ernzerhof M 1996 Generalized Gradient Approximation Made Simple *Phys. Rev. Lett.* **77** 3865–8
- [36] Grimme S 2006 Semiempirical GGA-type density functional constructed with a long-range dispersion correction *J. Comput. Chem.* **27** 1787–99
- [37] Monkhorst H J and Pack J D 1976 Special points for Brillouin-zone integrations *Phys. Rev. B* **13** 5188–92
- [38] Roundy D and Cohen M L 2001 Ideal strength of diamond, Si, and Ge *Phys. Rev. B* **64** 212103
- [39] Luo W, Roundy D, Cohen M L and Morris J W 2002 Ideal strength of bcc molybdenum and niobium *Phys. Rev. B* **66** 094110
- [40] Wei Q and Peng X 2014 Superior mechanical flexibility of phosphorene and few-layer black phosphorus *Appl. Phys. Lett.* **104** 251915
- [41] Hu W and Yang J 2015 Defects in Phosphorene *J. Phys. Chem. C* **119** 20474–80

- [42] Ding Y and Wang Y 2015 Structural, Electronic, and Magnetic Properties of Adatom Adsorptions on Black and Blue Phosphorene: A First-Principles Study *J. Phys. Chem. C* **119** 10610–22
- [43] Brown A and Rundqvist S 1965 Refinement of the crystal structure of black phosphorus *Acta Crystallogr.* **19** 684–5
- [44] Go J, Bg B, H T, Wj M and Ra S 1995 Comparison of Cluster and Infinite Crystal Calculations on Zeolites with the Electronegativity Equalization Method (Eem) *J. Phys. Chem.* **99** 3251–8
- [45] Jones R O and Hohl D 1990 Structure of phosphorus clusters using simulated annealing—P2 to P8 *J. Chem. Phys.* **92** 6710–21
- [46] Pauling L and Simonetta M 1952 Bond Orbitals and Bond Energy in Elementary Phosphorus *J. Chem. Phys.* **20** 29
- [47] Osman R, Coffey P and Van Wazer J R 1976 Use of pseudopotential theory to study molecular structure. II. NOCOR (neglect of core orbitals) calculation of the P4 and P2 molecules and their interconversion *Inorg. Chem.* **15** 287–292
- [48] Plimpton S 1995 Fast Parallel Algorithms for Short-Range Molecular Dynamics *J. Comput. Phys.* **117** 1–19
- [49] Nos é S 1984 A unified formulation of the constant temperature molecular dynamics methods *J. Chem. Phys.* **81** 511–519
- [50] Hoover W G 1985 Canonical dynamics: Equilibrium phase-space distributions *Phys. Rev. A* **31** 1695–7
- [51] Vilhelmsen L B and Hammer B 2014 A genetic algorithm for first principles global structure optimization of supported nano structures *J. Chem. Phys.* **141** 044711
- [52] Dittner M, Müller J, Aktulga H M and Hartke B 2015 Efficient global optimization of reactive force-field parameters *J. Comput. Chem.* **36** 1550–1561
- [53] Rossini F D and Rossini F D 1952 *Selected values of chemical thermodynamic properties* vol 500 (US Government Printing Office Washington, DC)
- [54] Freysoldt C, Grabowski B, Hickel T, Neugebauer J, Kresse G, Janotti A and Van de Walle C G 2014 First-principles calculations for point defects in solids *Rev. Mod. Phys.* **86** 253–305

- [55] Komsa H-P, Kotakoski J, Kurasch S, Lehtinen O, Kaiser U and Krasheninnikov A V 2012 Two-Dimensional Transition Metal Dichalcogenides under Electron Irradiation: Defect Production and Doping *Phys. Rev. Lett.* **109** 035503
- [56] Hao F and Chen X 2016 First-principles study of the defected phosphorene under tensile strain *J. Appl. Phys.* **120** 165104

Figures

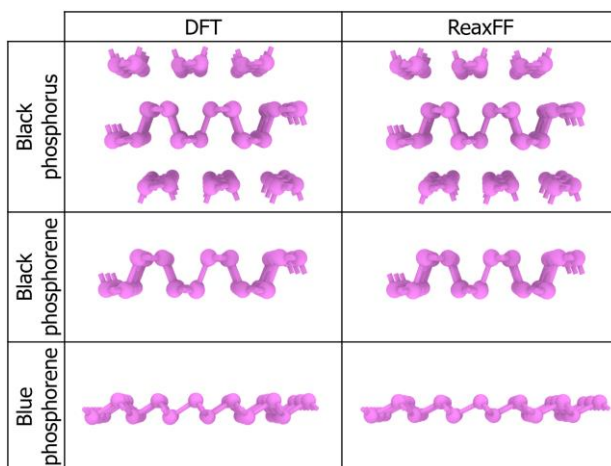


Fig. 1. Crystal structures of bulk black phosphorus, black phosphorene and blue phosphorene calculated by DFT and ReaxFF.

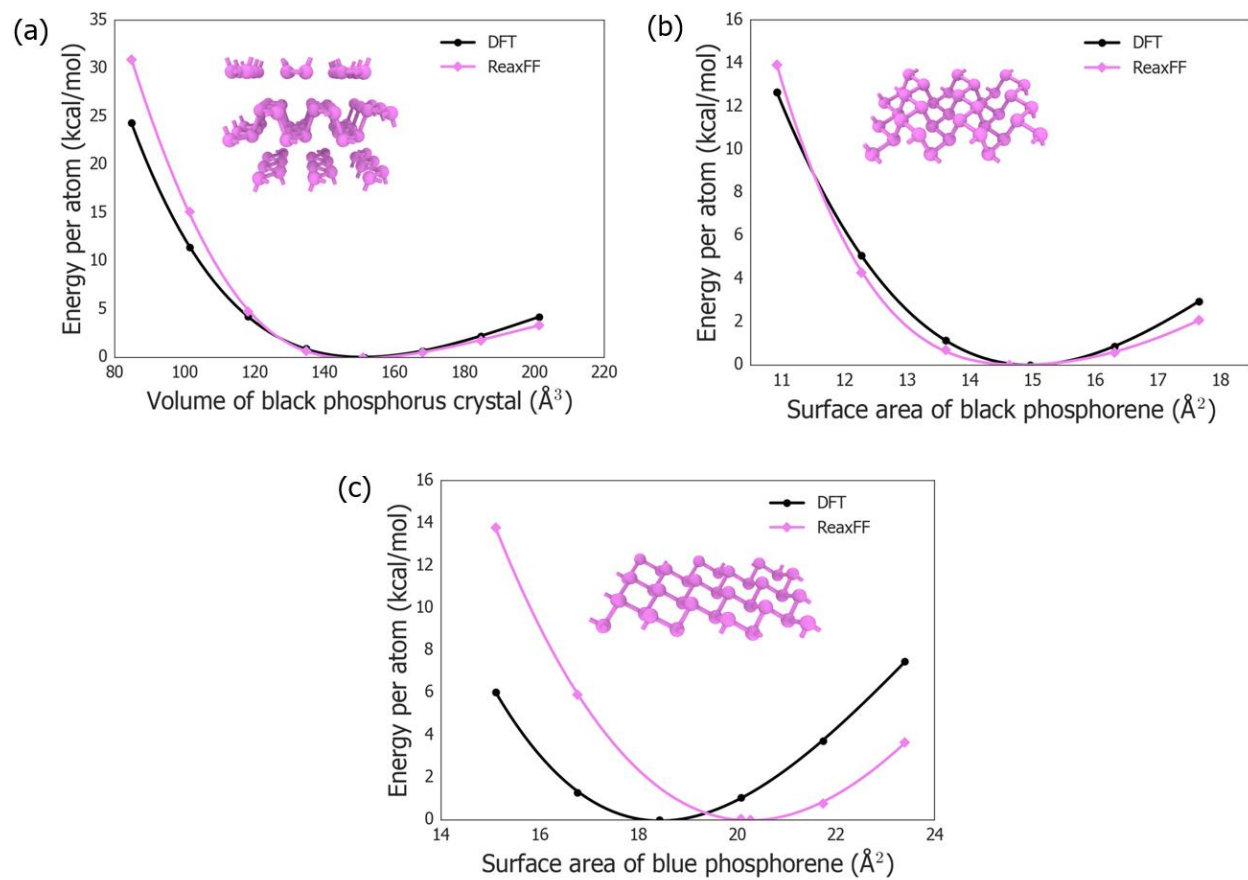


Fig. 2. Relative stabilities of (a) bulk black phosphorus for a broad range of unit cell volume, (b) black phosphorene for a broad range of in-plane unit cell area, (c) blue phosphorene for a broad range of in-plane unit cell area.

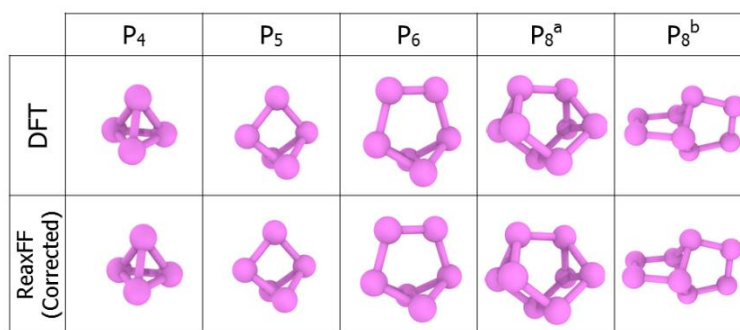


Fig. 3. Structures of phosphorus clusters from DFT and ReaxFF with the 60 ° correction.

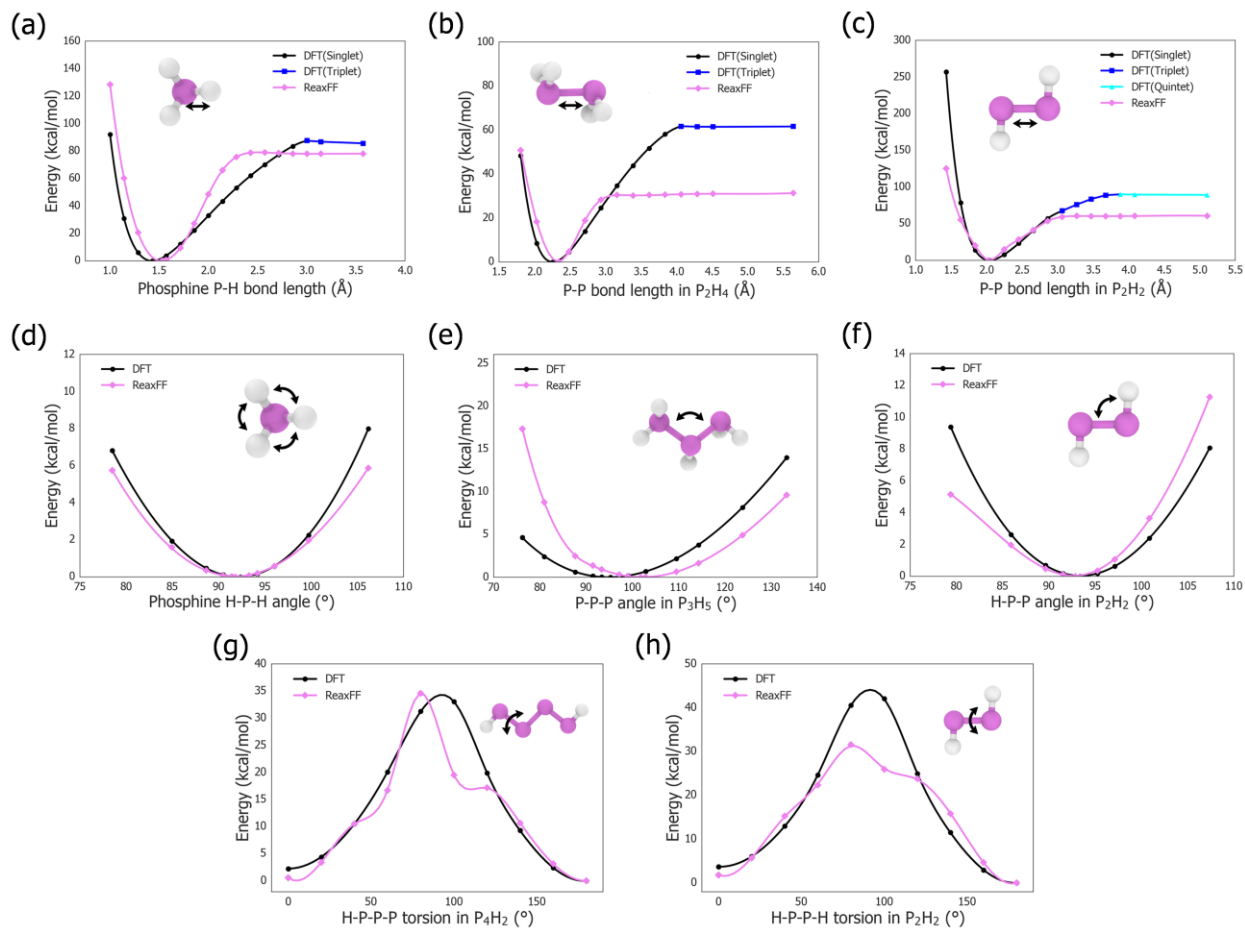


Fig. 4. DFT and ReaxFF potential energy curves for: (a) dissociation of a P-H bond in phosphine, (b) dissociation of a P-P bond in the P_2H_4 molecule, (c) dissociation of a P-P bond in the P_2H_2 molecule, (d) angle distortion of H-P-H in phosphine, (e) angle distortion of P-P-P in the P_3H_5 molecule, (f) angle distortion of H-P-P in the P_2H_2 molecule, (g) torsion distortion of H-P-P-P in the P_4H_2 molecule and of H-P-P-H in the P_2H_4 molecule.

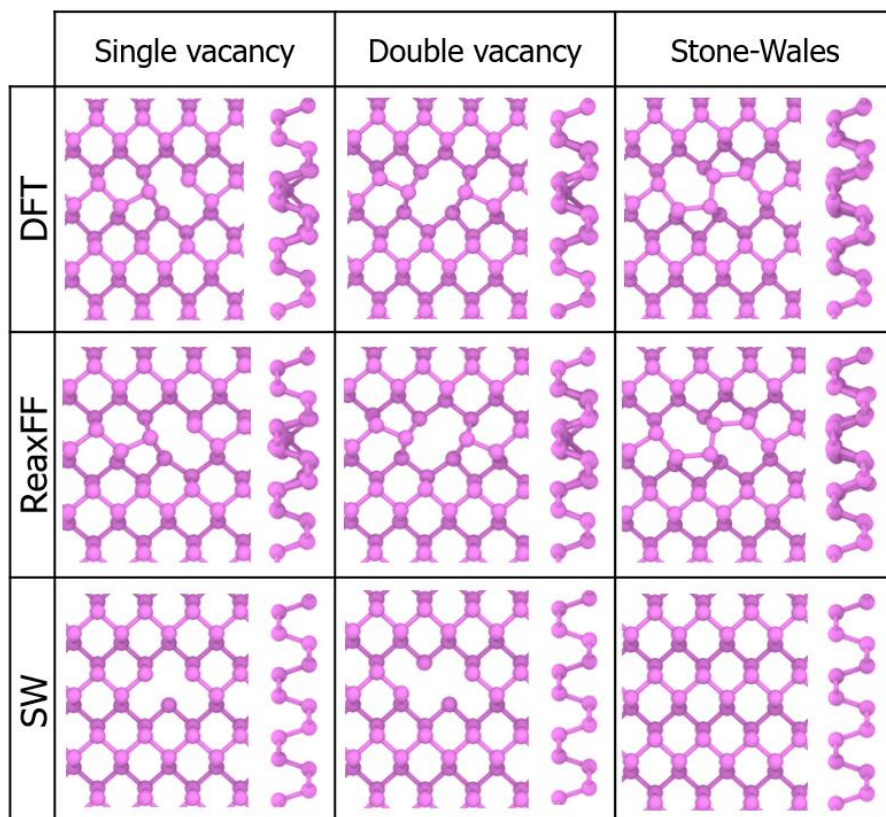


Fig. 5. Structures of defected black phosphorene calculated with DFT, ReaxFF and SW potential [1].

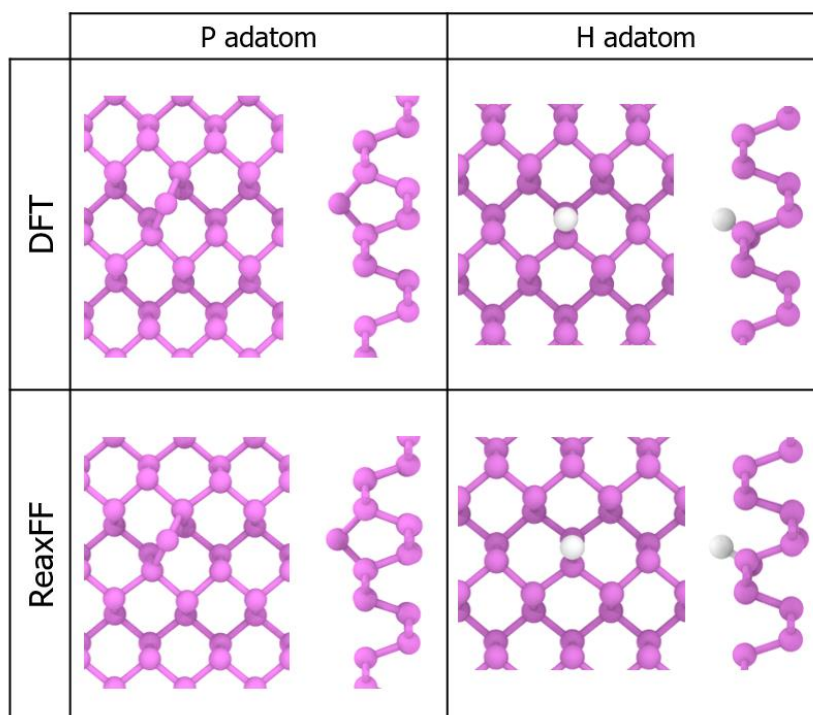


Fig. 6. Adsorption structures of P and H adatoms on black phosphorene calculated with DFT and ReaxFF.

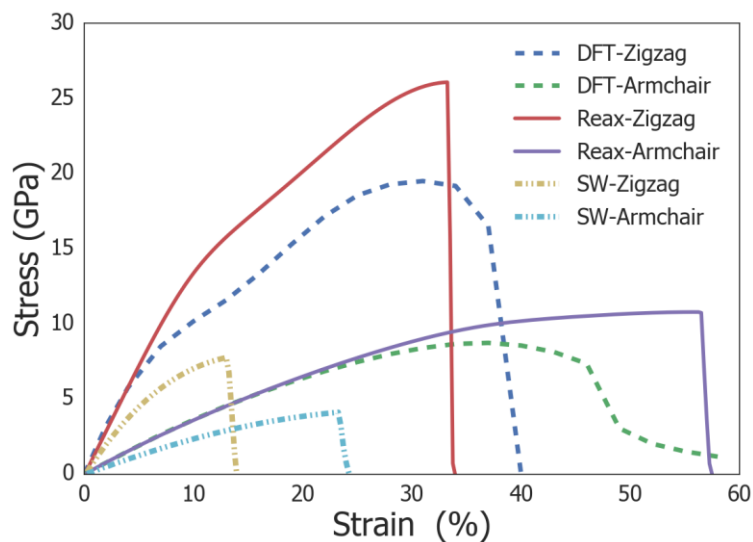


Fig. 7. Stress-strain responses of black phosphorene along the armchair direction and zigzag direction calculated by ReaxFF and SW potential at 1 K compared to DFT results.

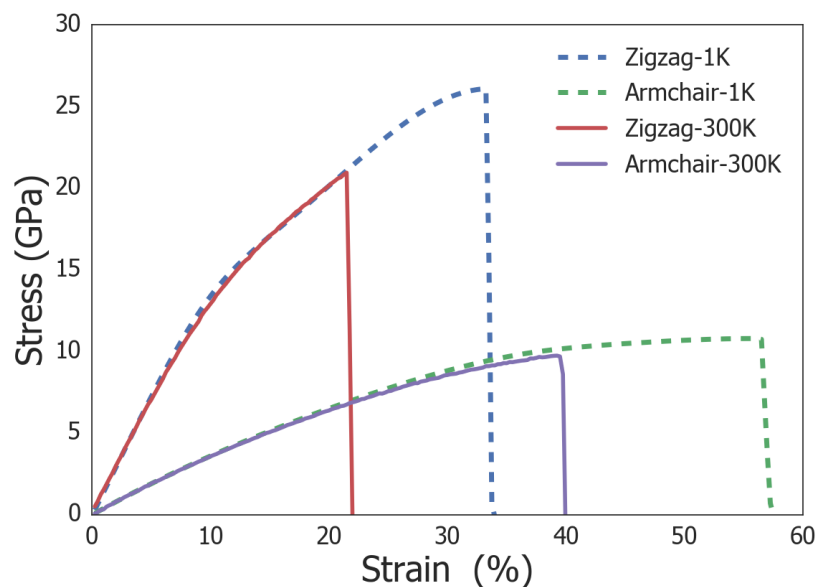


Fig. 8. Stress-strain responses of black phosphorene along the armchair direction and zigzag direction calculated by ReaxFF at 1K and 300 K.

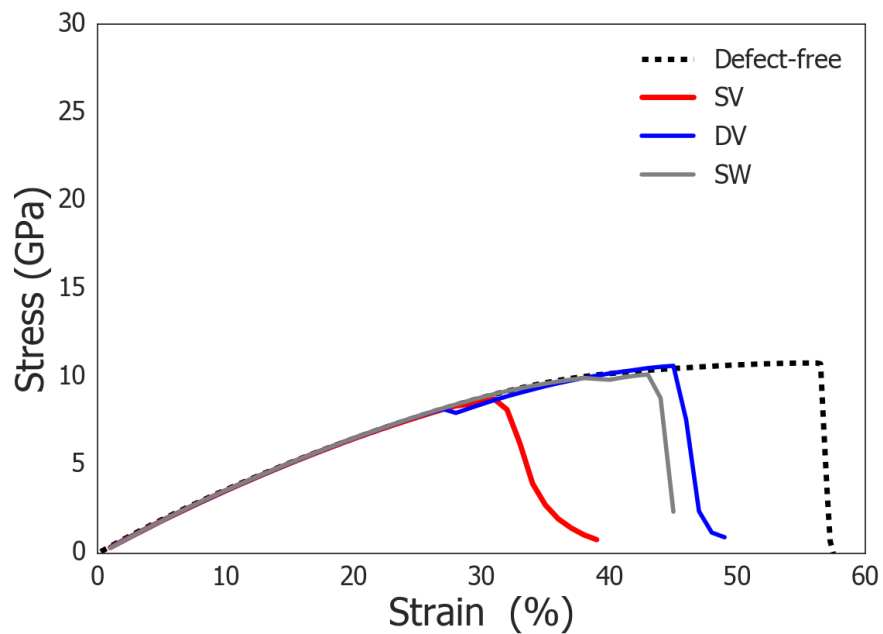


Fig. 9. Stress-strain responses of black phosphorene with defects along the armchair direction calculated by ReaxFF at 1K.

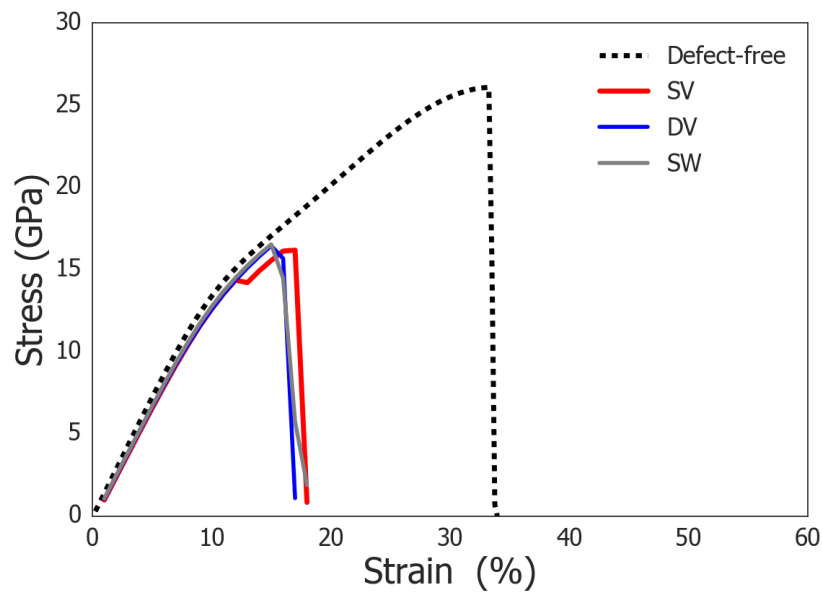


Fig. 10. Stress-strain responses of black phosphorene with defects along the zigzag direction calculated by ReaxFF at 1K.

Tables

Table 1

Atom parameters for P and H

	Bond radii				Coulomb parameters			Bond order correction			Valence Angle	
	r_{σ} (Å)	r_{π} (Å)	$r_{\pi\pi}$ (Å)	p_{ovun2}	η (eV)	χ (eV)	γ (Å)	p_{boc3}	p_{boc4}	p_{boc5}	p_{val3}	p_{val5}
P	2.1199	1.9507	1.8354	-2.0858	6.5970	4.8400	0.5751	15.5783	11.8556	2.8491	4.8954	1.6350
H	0.8873			-15.7683	10.5896	3.5768	0.6883	2.1457	1.3986	0.0003	2.1488	2.8793

For H, parameters from Ref. [31] were used. Definitions of the individual ReaxFF parameters in this table and Tables 2–6 can be found in Refs. [25,26,30].

Table 2

vdW parameters and low-gradient vdW correction parameters for P and H

	van der Waals parameters					lgvdW			
	r_{vdW} (Å)	ϵ (kcal/mol)	α	γ_{vdW} (Å)	r_{core} (Å)	ϵ_{core} (kcal/mol)	α_{core}	r_{lg} (Å)	C_{lg}
P	2.3355	0.0887	9.5120	7.6148	2.6552	0.0743	15.5028	2.1233	5066.5788
H	1.5420	0.0598	8.1910	30.9706	1.0000	0.0000	10.0000	1.9593	0.0001

For H, parameters from Ref. [31] were used.

Table 3

van der Waals and bond radius parameters for the P-H bond

	r_{σ} (Å)	r_{vdW} (Å)	ϵ (kcal/mol)	γ_{vdW} (Å)
P-H	1.3346	1.6594	0.2623	10.1613

Table 4

Bond energy and bond-order parameters for the P-P, P-H and H-H bonds

Bond	D_e^σ (kcal/mol)	D_e^π (kcal/mol)	$D_e^{\pi\pi}$ (kcal/mol)	p_{be1}	p_{be2}	p_{ovun1}	p_{bo1}	p_{bo2}	p_{bo3}	p_{bo4}	p_{bo5}	p_{bo6}
P-P	53.1210	23.8731	20.3604	0.4917	1.4218	0.4412	-0.2457	7.5884	-0.2226	13.6705	-0.2395	17.8190
P-H	207.1804			-0.2721	8.7816	0.5975	-0.1191	6.2022				
H-H	168.2342			-0.2191	6.1152	1.0062	-0.0889	6.0000				

For the H-H bond, parameters from Ref. [31] were used.

Table 5

Valence angle parameters.

Valence angle	θ_{00} (degree)	k_a (kcal/mol)	k_b (1/rad) ²	p_{v1}	p_{v2}
P-P-P	81.1291	81.4496	0.5055	0.1993	1.0534
H-P-P	90.2986	51.4268	1.5123	1.9661	2.6595
H-P-H	90.7891	8.9730	3.9682	0.3323	1.7123

Table 6

60 ° angle correction	θ_{60} (degree)	p_{cor1} (kcal/mol)	p_{cor2} (1/rad) ²	p_{cor3}
P-P-P	60	16.7000	150.0000	1.0534

The parameters of 60 °angle correction for P-P-P are designed to improve the description of phosphorus clusters with ReaxFF, explained in section 2.2.

Table 7

Torsion angle parameters

General parameters	Torsion angle	V_1	V_2	V_3	p_{tor1}
p_{tor2} 5.7863					
p_{tor3} 22.5238	H-P-P-P	-0.0611	34.4959	0.3329	-2.0854

p_{tor4}	5.3140	H-P-P-H	-0.1705	49.6594	1.5005	-2.5612
------------	--------	---------	---------	---------	--------	---------

Table 8

DFT results and ReaxFF results (at 0 K) compared to experimental obtained lattice constants of bulk black phosphorus, black phosphorene and blue phosphorene

Structure	Lattice parameter	DFT (Å)	ReaxFF (Å)	Experiment (Å)
Bulk black phosphorus	a	3.30	3.43	3.31 [43]
	b	4.40	4.26	4.38 [43]
	c	10.43	10.33	10.48 [43]
Black phosphorene	a	3.28	3.44	
	b	4.56	4.29	
Blue phosphorene	a	3.26	3.42	
	b	5.65	5.93	

Table 9

DFT results versus ReaxFF results of cohesive energies compared to SW results and experimental data

Structure	Property	DFT	ReaxFF	SW	Experiment
Bulk black phosphorus	$E_{cohesive}(\text{bulk})/\text{eV}$	-3.43	-2.91		-3.26 [53]
Black phosphorene	$E_{cohesive}(\text{black})/\text{eV}$	-3.35	-2.84	-0.54 [1]	
	$E_{cohesive}(\text{black}) - E_{cohesive}(\text{bulk}) / (\text{kcal/mol})$	1.94	1.64		
Blue phosphorene	$E_{cohesive}(\text{blue}) - E_{cohesive}(\text{bulk}) / (\text{kcal/mol})$	3.00	2.18		

$E_{cohesive}(\text{bulk})$, $E_{cohesive}(\text{black})$ and $E_{cohesive}(\text{blue})$ are the cohesive energies of bulk black phosphorus, black phosphorene and blue phosphorene, respectively.

Table 10

Formation energy per atom of phosphorus clusters calculated by ReaxFF (with or without 60 ° correction) compared to DFT results.

Cluster	Formation energy per atom (kcal/mol)		
	DFT	ReaxFF	ReaxFF (60 ° correction)
P ₄	7.6	56.9	7.6
P ₅	14.3	30.7	12.6
P ₆	11.3	25.1	9.5
P ₈ ^a	8.2	18.5	6.2
P ₈ ^b	12.7	11.1	11.9

Table 11

DFT results versus ReaxFF results of formation energies of SV, DV and SW defects in black phosphorene compared to SW results.

Defect	Defect formation energy (eV)		
	DFT	ReaxFF	SW [1]
SV	1.66	1.85	0.54
DV	1.95	2.48	0.73
SW	1.42	1.88	0.00

Table 12

DFT results versus ReaxFF results of binding energies of phosphorus and hydrogen adatoms in black phosphorene.

Atom	Adatom energy (eV)	
	DFT	ReaxFF
P	1.67	1.19
H	0.73	0.76

Table 13

DFT results versus ReaxFF results of Young's modulus of black phosphorene in armchair and zigzag directions compared to SW results.

	DFT	ReaxFF	SW [1]
E_{arm} (GPa)	37.8	39.3	33.5
E_{zig} (GPa)	160.4	146.8	105.5
$E_{\text{zig}} / E_{\text{arm}}$	4.24	3.73	3.15

P-H ReaxFF parameters (without 60 degree correction):

```

Reactive MD-force field
39      ! Number of general parameters
50.0000 !Comment here
9.5469 !Comment here
26.5405 !Comment here
1.7224 !Comment here
6.8702 !Comment here
60.4850 !Comment here
1.0588 !Comment here
4.6000 !Comment here
12.1176 !Comment here
13.3056 !Comment here
-70.5044 !Comment here
0.0000 !Comment here
10.0000 !Comment here
2.8793 !Comment here
33.8667 !Comment here
6.0891 !Comment here
1.0563 !Comment here
2.0384 !Comment here
6.1431 !Comment here
6.9290 !Comment here
0.3842 !Comment here
2.9294 !Comment here
-2.4837 !Comment here
5.7863 !Comment here
22.5238 !Comment here
5.3140 !Comment here
-1.2327 !Comment here
2.1645 !Comment here
1.5591 !Comment here
0.1000 !Comment here
2.1365 !Comment here
0.6991 !Comment here
50.0000 !Comment here
1.8512 !Comment here
0.5000 !Comment here
1.0000 !Comment here
5.0000 !Comment here
0.0000 !Comment here
2.6962 !Comment here
2      !Nr of atoms; cov.r; valency;a.m;Rvdw;Evdw;gammaEEM;cov.r2;
      !alfa;gammaW;valency;Eunder;Eover;chiEEM;etaEEM;n.u.
      !cov r3;Elp;Heat inc.;n.u.;n.u.;n.u.;n.u.
      !ov/un;val1;n.u.;val3,vval4
P      2.1199 3.0000 30.9738 2.3355 0.0887 0.5751 1.9507 5.0000
      9.5120 7.6148 3.0000 0.0000 82.5172 4.8400 6.5970 0.0000
      1.8354 0.0000 120.0000 11.8556 15.5783 2.8491 5066.5788 2.1233
      -2.0858 4.8954 1.0338 3.0000 1.6350 2.6552 0.0743 15.5028
      5066.5788 2.1233
H      0.8873 1.0000 1.0080 1.5420 0.0598 0.6883 -0.1000 1.0000
      8.1910 30.9706 1.0000 0.0000 121.1250 3.5768 10.5896 1.0000
      -0.1000 0.0000 54.0596 1.3986 2.1457 0.0003 0.0001 1.9593
      -15.7683 2.1488 1.0338 1.0000 2.8793 2.0000 0.0000 10.0000
      0.0001 1.9593
3      ! Nr of bonds; Edis1;LPpen;n.u.;pbe1;pbo5;l3corr;pbo6

```

```

pbe2;pbo3;pbo4;n.u.;pbo1;pbo2;ovcorr
1 1 53.1210 23.8731 20.3604 0.4917 -0.2395 1.0000 17.8190 0.4412
1.4218 -0.2226 13.6705 1.0000 -0.2457 7.5884 1.0000 0.0000
1 2 207.1804 0.0000 0.0000 -0.2721 0.0000 1.0000 6.0000 0.5975
8.7816 1.0000 0.0000 1.0000 -0.1191 6.2022 0.0000 0.0000
2 2 168.2342 0.0000 0.0000 -0.2191 0.0000 1.0000 6.0000 1.0062
6.1152 1.0000 0.0000 1.0000 -0.0889 6.0000 0.0000 0.0000
1 !Nr of off-diagonal terms; Ediss;Ro;gamma;rsigma;rpi;rpi2
1 2 0.2623 1.6594 10.1613 1.3346 -1.0000 -1.0000
6 !Nr of angles;at1;at2;at3;Thetao,o;ka;kb;pv1;pv2
1 1 1 81.1291 81.4496 0.5055 0.0000 0.1993 0.000 1.0534
2 2 2 0.0000 0.0000 5.8635 0.0000 0.0000 0.0000 1.0400
2 1 1 90.2986 51.4268 1.5123 0.0000 1.9661 0.0000 2.6595
2 1 2 90.7891 8.9730 3.9682 0.0000 0.3323 0.0000 1.7123
1 2 1 7.0790 0.0000 0.4358 0.0000 0.0000 0.1050 2.1684
2 2 1 0.0000 0.0000 6.0000 0.0000 0.0000 0.0000 1.0400
2 !Nr of torsions;at1;at2;at3;at4;V1;V2;V3;V2(BO);vconj;n.u;n
1 1 1 2 -0.0611 34.4959 0.3329 -2.0854 0.0000 0.0000 0.0000
2 1 1 2 -0.1705 49.6594 1.5005 -2.5612 0.0000 0.0000 0.0000
0 !Nr of hydrogen bonds;at1;at2;at3;Rhb;Dehb;vhl

```

P-H ReaxFF parameters (with 60 degree correction):

```

Reactive MD-force field
39 !Number of general parameters
50.0000 !Comment here
9.5469 !Comment here
26.5405 !Comment here
1.7224 !Comment here
6.8702 !Comment here
60.4850 !Comment here
1.0588 !Comment here
4.6000 !Comment here
12.1176 !Comment here
13.3056 !Comment here
-70.5044 !Comment here
0.0000 !Comment here
10.0000 !Comment here
2.8793 !Comment here
33.8667 !Comment here
6.0891 !Comment here
1.0563 !Comment here
2.0384 !Comment here
6.1431 !Comment here
6.9290 !Comment here
0.3842 !Comment here
2.9294 !Comment here
-2.4837 !Comment here
5.7863 !Comment here
22.5238 !Comment here
5.3140 !Comment here
-1.2327 !Comment here
2.1645 !Comment here
1.5591 !Comment here
0.1000 !Comment here
2.1365 !Comment here
0.6991 !Comment here
50.0000 !Comment here
1.8512 !Comment here
0.5000 !Comment here
1.0000 !Comment here
5.0000 !Comment here
0.0000 !Comment here
2.6962 !Comment here
2 !Nr of atoms; cov.r; valency;a.m;Rvdw;Evdw;gammaEEM;cov.r2;
alfa;gammavdW;valency;Eunder;Eover;chiEEM;etaEEM;n.u.
cov r3;Elp;Heat inc;n.u.;n.u.;n.u.;n.u.
ov/un;val1;n.u.;val3,vval4
P 2.1199 3.0000 30.9738 2.3355 0.0887 0.5751 1.9507 5.0000
9.5120 7.6148 3.0000 0.0000 82.5172 4.8400 6.5970 0.0000
1.8354 0.0000 120.0000 11.8556 15.5783 2.8491 5066.5788 2.1233
-2.0858 4.8954 1.0338 3.0000 1.6350 2.6552 0.0743 15.5028
5066.5788 2.1233
H 0.8873 1.0000 1.0080 1.5420 0.0598 0.6883 -0.1000 1.0000
8.1910 30.9706 1.0000 0.0000 121.1250 3.5768 10.5896 1.0000
-0.1000 0.0000 54.0596 1.3986 2.1457 0.0003 0.0001 1.9593
-15.7683 2.1488 1.0338 1.0000 2.8793 2.0000 0.0000 10.0000
0.0001 1.9593
3 !Nr of bonds; Edis1;LPpen;n.u.;pbe1;pbo5;l3corr;pbo6
pbe2;pbo3;pbo4;n.u.;pbo1;pbo2;ovcorr
1 1 53.1210 23.8731 20.3604 0.4917 -0.2395 1.0000 17.8190 0.4412
1.4218 -0.2226 13.6705 1.0000 -0.2457 7.5884 1.0000 0.0000
1 2 207.1804 0.0000 0.0000 -0.2721 0.0000 1.0000 6.0000 0.5975
8.7816 1.0000 0.0000 1.0000 -0.1191 6.2022 0.0000 0.0000
2 2 168.2342 0.0000 0.0000 -0.2191 0.0000 1.0000 6.0000 1.0062
6.1152 1.0000 0.0000 1.0000 -0.0889 6.0000 0.0000 0.0000

```

```

1  ! Nr of off-diagonal terms; Ediss;Ro;gamma;rsigma;rpi;rpi2
1 2 0.2623 1.6594 10.1613 1.3346 -1.0000 -1.0000
7  ! Nr of angles;at1;at2;at3;Thetao.o;ka;kb;pv1;pv2
1 1 1 60.0000 16.7000 150.000 0.0000 0.1993 0.0000 1.0534
1 1 1 81.1291 81.4496 0.5055 0.0000 0.1993 0.0000 1.0534
2 2 2 0.0000 0.0000 5.8635 0.0000 0.0000 0.0000 1.0400
2 1 1 90.2986 51.4268 1.5123 0.0000 1.9661 0.0000 2.6595
2 1 2 90.7891 8.9730 3.9682 0.0000 0.3323 0.0000 1.7123
1 2 1 7.0790 0.0000 0.4358 0.0000 0.0000 0.1050 2.1684
2 2 1 0.0000 0.0000 6.0000 0.0000 0.0000 0.0000 1.0400
2  ! Nr of torsions;at1;at2;at3;at4;V1;V2;V3;V2(BO);vconj;n.u;n
1 1 1 2 -0.0611 34.4959 0.3329 -2.0854 0.0000 0.0000 0.0000
2 1 1 2 -0.1705 49.6594 1.5005 -2.5612 0.0000 0.0000 0.0000
0  ! Nr of hydrogen bonds;at1;at2;at3;Rhb;Dehb;vhb1

```